



Published in final edited form as:

Anal Chem. 2010 December 1; 82(23): 9727–9735. doi:10.1021/ac101843n.

Ligase Detection Reaction Generation of Reverse Molecular Beacons for Near Real-Time Analysis of Bacterial Pathogens Using Single-Pair Fluorescence Resonance Energy Transfer and a Cyclic Olefin Copolymer Microfluidic Chip

Zhiyong Peng,

Department of Chemistry, Louisiana State University, Baton Rouge, Louisiana, United States

Steven A. Soper*,

Departments of Chemistry and Mechanical Engineering, Louisiana State University, Baton Rouge, Louisiana, United States, and Nano-BioTechnology and Chemical Engineering, Ulsan National Institute of Science and Technology, Ulsan, South Korea

Maneesh R. Pingle,

Department of Microbiology, Weill Medical College of Cornell University, New York, New York, United States

Francis Barany, and

Department of Microbiology, Weill Medical College of Cornell University, New York, New York, United States

Lloyd M. Davis

Center for Laser Applications, University of Tennessee Space Institute, Tullahoma, Tennessee, United States

Abstract

Detection of pathogenic bacteria and viruses require strategies that can signal the presence of these targets in near real-time due to the potential threats created by rapid dissemination into water and/or food supplies. In this paper, we report an innovative strategy that can rapidly detect bacterial pathogens using reporter sequences found in their genome without requiring polymerase chain reaction (PCR). A pair of strain-specific primers was designed based on the 16S rRNA gene and were end-labeled with a donor (Cy5) or acceptor (Cy5.5) dye. In the presence of the target bacterium, the primers were joined using a ligase detection reaction (LDR) only when the primers were completely complementary to the target sequence to form a reverse molecular beacon (rMB), thus bringing Cy5 (donor) and Cy5.5 (acceptor) into close proximity to allow fluorescence resonance energy transfer (FRET) to occur. These rMBs were subsequently analyzed using single-

© 2010 American Chemical Society

*To whom correspondence should be addressed. chsoper@lsu.edu.

SUPPORTING INFORMATION AVAILABLE

Design and operation of the COC chip, secondary structure analysis of the rMB, electrophoresis results for PCR and LDR analysis, and details of different linker structures for donor/ acceptor attachment and autofluorescence background for different polymers. This material is available free of charge via the Internet at <http://pubs.acs.org>.

molecule detection of the FRET pairs (single-pair FRET; spFRET). The LDR was performed using a continuous flow thermal cycling process configured in a cyclic olefin copolymer (COC) microfluidic device using either 2 or 20 thermal cycles. Single-molecule photon bursts from the resulting rMBs were detected on-chip and registered using a simple laser-induced fluorescence (LIF) instrument. The spFRET signatures from the target pathogens were reported in as little as 2.6 min using spFRET.

Each year in the United States, the number of illnesses associated with bacterial contamination of consumer food products is estimated to be as high as 5 million cases causing more than 4500 deaths according to the USDA.¹ Therefore, the rapid and highly specific identification of potential pathogenic contaminations are significant for maintaining public health and safety by minimizing the spread of the contamination.²⁻⁵

Conventional culture-based methods for pathogen detection are labor-intensive and time-consuming with a minimum of 2 days required for identification of the suspect bacteria, and also, interpretation is prone to human error.⁶ Immunoassays are an attractive alternative due to the highly selective antigen-antibody interactions they afford. In addition, immunoassays can be applied to complex biological matrixes with little sample preparation,^{7,8} as well as the ability to perform parallel analyses.^{9,10} However, some target bacteria cannot be easily identified via an immunoassay due to difficulties associated with finding appropriate monoclonal antibodies to impart the necessary specificity for particular strains.¹¹

Genome-specific identification utilizes unique reporter sequences within the genome of the target pathogen. In most cases, a polymerase chain reaction (PCR) is used to generate sufficient copies of the target sequence to aid in detection. The PCR amplicons can be subjected to an electrophoretic separation¹² or liquid chromatography¹³ for identifying the bacterium. Due to the high sensitivity and specificity of PCR, it has been widely used to detect trace amounts of microorganisms in many scenarios, such as monitoring water quality,¹⁴ food contamination,⁴ and infectious biological agents.⁵ When different primer pairs within the same reaction chamber are incorporated, PCR has multiplexing capabilities as well to allow for the analysis of as many as 10 different pathogens.^{13,15,16} Mathies's group recently reported a capillary electrophoresis-based microanalysis system to perform cell pre-concentration, purification, and PCR for pathogen analysis.¹⁷ This system could detect *E. coli* O157:H7 with a detection limit of 0.2 cfu/ μ L in a processing time of >73 min.

Optical biosensors have also been reported for pathogen analysis using different transduction modalities.¹⁸⁻²⁵ Rider et al.²⁶ showed the recognition of biopathogenic species using a B lymphocyte cell line engineered to express both a bioluminescent protein and pathogen-specific membrane-bound antibodies. Low levels of certain pathogens were detected through binding to the antibodies of the B cells and, thus, triggering the bioluminescent protein to emit light; 50 cfu of *Yersinia pestis* could be detected with a total processing time of ~3 min.

While the aforementioned techniques can be viewed as effective tools for monitoring the presence of certain bacterial species from a number of different sample inputs, they do possess limitations. For example, PCR-based schemes need several hours to obtain the

required results. Even real-time PCR has turnaround times of 20–30 min due to the high number of thermal cycles employed, especially for cases where the bacterial copy number found in the sample can be low. In addition, PCR techniques are limited in terms of their specificity because different strains may possess single base variations in their genetic sequence, which is difficult to register via PCR. For example, *B. anthracis* has been discovered to possess ~3500 different single nucleotide variations among its eight strains,²⁷ and application of PCR-based biosensing becomes impractical to identify the specific strain in a timely manner.

In contrast to PCR, the ligase detection reaction (LDR) can offer superior sequence specificity even for single base variations.²⁸ In the LDR assay, a successful ligation event between two designed primers (common and discriminating primer) can occur only if they are completely complementary to the target DNA, especially at the 3'-end of the discriminating primer.²⁹ The reaction can distinguish specific sequence variations even in the presence of a majority of DNA that does not possess the variation.

In this study, single-pair fluorescence resonance energy transfer (FRET) was coupled to an LDR to provide near real-time readout of different bacterial pathogenic species with high strain specificity. LDR thermal cycling and single-molecule readout were carried out directly on a thermoplastic microfluidic device to provide rapid assay results. The assay strategy (LDR-single-pair FRET; spFRET) for strain-specific identification of bacterial species is illustrated in Figure 1. A similar assay was adopted by Wabuye et al. for detecting single nucleotide mutations in *KRAS* genes.³⁰ In this assay, a discriminating primer and a common primer were designed based on the sequence of a reporter region within the genome of the bacterial target. These primers also contained a 10-base arm with sequences that were complementary to each other and were covalently attached to a donor and acceptor fluorophore. Successful ligation of the primers will occur only if the complementary sequence is contained within the target generating a reverse molecular beacon (rMB), bringing the donor and acceptor dyes into close proximity producing a FRET response. Because the arm sequences of the rMB were designed to possess a higher melting temperature (T_m) and, thus, were thermodynamically more stable than the target-oligonucleotide duplex, the rMB reorganized itself into a stable stem-loop conformation following ligation. The LDR was carried out directly on genomic DNA isolated from lysed bacterial cells with no PCR required, and direct quantification was accomplished using single-molecule counting. The lack of a primary PCR step significantly reduced the assay turnaround time, providing near real-time readout. In contrast to that previously reported using this assay for detecting single nucleotide variations in *KRAS* genes,³⁰ the genome of bacteria usually possesses sporadic sequence variations at multiple sites and not at a single location. Therefore, the present format of this LDR-spFRET assay did not depend on a single point mutation at the 3'-end of the discriminating primers but multiple mismatches between the discriminating and common primers used for the LDR and the target genomic DNA isolated from the bacterial species. This should result in improved specificity due to differences in the T_m of the matched and mismatched duplexes (LDR primers and target genomic DNA) in addition to a possible mismatch at the ligation site.

Two Gram-positive (Gram(+)) pathogens, *S. aureus subsp. aureus* and *S. epidermidis* RP-62A, and one Gram-negative bacterium (Gram(-)), *E. coli* K-12, were employed in this work as models. *S. aureus* is an aggressive pathogen responsible for a range of acute and pyogenic infections, and *S. epidermidis* is primarily associated with infections produced from such devices as implanted prosthetic joints or heart valves.^{31,32} *E. coli* K-12 is a strain of bacteria with little harm to humans, but members of its family can be very harmful, such as *E. coli* O157:H7.

EXPERIMENTAL SECTION

Materials and Reagents

The oligonucleotide primers required for the LDR were synthesized by Integrated DNA Technologies (IDT, Coralville, IA), purified by RP-HPLC, and suspended in 1× TE buffer. *Thermus aquaticus* (Taq) DNA ligase was purchased from New England Biolabs (Beverly, MA). AmpliTaq Gold polymerase was purchased from Applied Biosystems (Foster City, CA). Cyclic olefin copolymer, COC, was purchased from Topas Advanced Polymers (Florence, Kentucky).

Bacterial Samples

Three bacterial strains, *Staphylococcus aureus subsp. aureus* (ATCC 700699), *Staphylococcus epidermidis* (ATCC 35984), and *Escherichia coli* K-12 (ATCC 700926) served as models for this study and were acquired from ATCC (Manassas, VA). A series of dilutions to produce the desired cell densities were made in 1× TE buffer consisting of each bacterial genomic DNA. The concentration of the DNA was examined with a UV/vis spectrophotometer (Ultrospec 4000, Amersham Bioscience) using the 260 nm/280 nm absorption ratio. The bacterial genomic DNA was stored at -20 °C until used.

Polymerase Chain Reaction and Ligase Detection Reaction

The PCR contained 1× PCR buffer II (Applied Biosystems), 2.5 mM MgCl₂, 200 μM dNTPs, 1 μM forward and reverse primers (see Table 1 for their sequences), 1.25 units of DNA polymerase (AmpliTaq Gold Polymerase, Applied Biosystems), ~10 ng of template DNA, and enough nuclease-free H₂O to make a total reaction volume of 50 μL. The PCR was run in a thermal cycling machine (Eppendorf MasterCycler, Hamburg, Germany) with polymerase added under hot start conditions. The reaction cocktail was subjected to 35 thermal cycles at 94 °C for 15 s, 60 °C for 1 min, 72 °C for 1 min, and a final extension at 72 °C for 7 min. The temperature was held at 99 °C to deactivate the polymerase enzyme prior to LDR.

Bench-top LDRs were carried out in 0.2 mL polypropylene microtubes using a benchtop thermal cycler (Eppendorf). The reaction cocktail consisted of 2 units/μL of thermostable DNA ligase, 20 mM Tris-HCl (pH 7.6), 25 mM potassium acetate, 10 mM magnesium acetate, 1 mM NAD⁺ cofactor, 10 mM dithiothreitol, 0.1% Triton X-100, 10 nM of each LDR primer, the appropriate amount of the DNA target, and nuclease-free H₂O to make a total reaction volume of ~20 μL. Prior to thermal cycling, the reaction was first heated to 94 °C to denature the DNA, followed by addition of the ligase enzyme. The reaction mixture

was processed using the appropriate number of thermal cycles (linear amplification of LDR products), each of which was composed of a denaturation step at 94 °C for 30 s and an annealing/ligation step at 65 °C for 2 min. The reaction was stopped by quickly cooling to 4 °C and adding 0.5 μ L of 0.5 M EDTA.

On-chip LDRs were similar to those noted for the benchtop reactions except that bovine serum albumin (BSA, 0.5 mg/mL) was included in the reaction mixture to minimize any potential nonspecific adsorption artifacts of the ligase enzyme onto the thermal reactor surface.^{33,34} Kapton heaters were attached directly to the bottom of the microchip to provide the required temperatures for on-chip LDR using a continuous flow reactor format (see below). All PCR and LDR products were verified using slab gel and capillary gel electrophoresis. See the Supporting Information for discussion of the experimental conditions and results for the electrophoresis.

Primer and rMB Design for the LDRs

In designing the oligonucleotide primers for the LDR-spFRET assay, the 16S rRNA gene was selected as the biomarker for bacteria identification due to its highly conserved sequence.^{6,32,35} Moreover, the 16S rRNA gene appears at multiple locations within the genome of each bacterial cell increasing its copy number and, thus, aiding detection. The sequence of the primers used for the PCRs and LDRs are listed in Table 1. Two regions within the 16S rRNA gene were interrogated. The PCR primers denoted “AMP1” and the LDR primer set denoted as “Gram+” were designed for one region of the 16S rRNA gene and used to differentiate Gram(+) from Gram(-) bacteria following the LDR. When the specific strain within the Gram(+) species needed to be identified, a second region of the 16S rRNA was used (see PCR primer sets “AMP2” in Table 1). The LDR primer pairs (see Table 1) denoted as “epid” were based on the region of the 16S rRNA gene used to identify *S. epidermidis*, and the LDR primer pairs denoted as “aureus” were designed to identify *S. aureus*.

The design of the rMB was assisted by the DNA folding program from IDT, which uses minimum free energy of formation to predict the T_m of duplexed DNA as well as any possible secondary structure(s). Figure S1 (see Supporting Information) shows the results of this analysis indicating that the rMB was the most thermodynamically favored conformation when folding was performed at 75 °C using the primer pairs selected for spFRET.

For differentiation between Gram(+) and Gram(-) bacteria, the discriminating primer was composed of a 20 base loop sequence and a 10 base stem sequence with the 5'-end of the stem labeled with Cy5.5. The 33 base common primer, which contained a 23 base loop sequence and a 10 base stem sequence, was phosphorylated at its 5'-end and Cy5-labeled at its 3'-end. In the presence of target DNA, the common primer and the discriminating primer both can hybridize to the target and undergo ligation but only if the primers are completely complementary to the target DNA. At the detection temperature employed, the ligated primers formed the rMB that provided a spectroscopic signature of the presence of the target through spFRET.

Measurement of Energy Transfer

To evaluate the design of the rMBs, the LDR products were examined in a fluorometer (FluoroLog 3, HORIBA Jobin Yvon, Edison, NJ) to determine the extent and efficiency of energy transfer. A Peltier heating unit was equipped with the fluorometer to allow spectral interrogation at 75 °C, which was below the T_m of the stem associated with the rMB (83.4 °C, see Supporting Information) but above the T_m of the unligated or ligated primers hybridizing to their complementary sequences in the target DNA at the concentrations employed for the LDR/spFRET assays. The sample was excited at 635 nm, and the emission was collected between 650 and 750 nm.

Fabrication of the COC Microfluidic Device

A complete description of the fabrication of the COC microfluidic chip and its operation can be found in the Supporting Information. In addition, a schematic of the fluidic chip can also be found in the Supporting Information (see Figure S2).

Instrumentation for Laser-Induced Fluorescence Single-Molecule Detection

LDR rMB products were measured using a laser-induced fluorescence (LIF) system. Briefly, a precollimated 635 nm diode laser (Model CPS196, Thorlabs, Newton, NJ) was used for excitation. The laser beam was conditioned using a laser line filter (640DF20, Omega, Brattleboro, VT) and directed by a dichroic mirror (690DRLP, Omega Optical) into a microscope objective (M-60X, NA = 0.85, Newport, Irvine, CA). The emitted fluorescence was then collected by the same objective and transmitted through a dichroic and pinhole (i.d. = 100 μ m). The fluorescence light was spectrally filtered using interference filters, including a long-pass filter (3RD690LP, Omega Optical) and a bandpass filter (HQ710/20 m, Chroma Technology, Rockingham, VT). Finally, the fluorescence was focused onto the active area of a single photon avalanche diode (SPCM-200, EG&G, Vandreuil, Canada) using a 10 \times microscope objective. The signal from the SPAD was transformed by a pulse converter into a TTL pulse and processed using a digital counting board (PCI-6602, National Instruments, Austin, TX).

Single-molecule fluorescence measurements were performed by measuring the time-of-arrival of single photon events. To accomplish this, a PCI-6602 data acquisition board provided 12.5 ns time resolution at its maximum clock frequency of 80 MHz. Each photon event was stamped with a time, which allowed binning the individual photon events into a user-defined bin.

RESULTS AND DISCUSSION

Assay Validation through PCR and LDR

To initially examine the design of the LDR primers and the rMB structure as well as the efficiency of the LDR, PCR was carried out on genomic DNA isolated from *S. aureus*, *S. epidermidis*, and *E. coli* to provide sufficient targets so that the products could be examined by gel electrophoresis and/or a conventional fluorometer. However, the PCR step was eliminated for the on-chip single-molecule detection experiments, which used genomic DNA as the LDR targets. Two different PCR amplicons were evaluated, both defined by the

primer sets listed in Table 1. Figure S3 (see Supporting Information) indicated successful PCRs using these primer sets with the proper amplicon sizes when performed in a uniplex or duplex format.

We then used these PCR amplicons as inputs for the evaluative LDR phases of this study. In these experiments, the LDR was run using 20 thermal cycles and the ratio of peak heights between the LDR product and unligated primers used to determine the LDR efficiency. From these measurements (see Figure S4(A), Supporting Information), the average LDR efficiency was estimated to be 40% for each thermal cycle (see Supporting Information for details).

LDR for Determining Gram(±) or Bacterial Strain

Figure S4(B) of the Supporting Information shows the results of a 20 cycle LDR run on PCR amplicons using primers (AMP1, see Table 1) based on the 16S rRNA gene geared for the identification of Gram(+) bacteria, *S. aureus* and *S. epidermidis*. LDR products were successfully detected for both, but no LDR products were found when *E. coli* was used as the target, consistent with the Gram(+) and Gram(−) nature of these species.

To distinguish between *S. aureus* and *S. epidermidis*, a strain-specific primer pair was used for the LDR that interrogated the section of the genome defined by PCR primer set AMP2 (see Table 1). Figures S4(C) and S4(D) (see Supporting Information) show the results of a 20 cycle LDR when the strain-specific primers were used for the LDR. As can be seen in Figure S4(C) (Supporting Information), when the primer pair specific for *S. aureus* was used, an LDR product was found for *S. aureus* only. Conversely, when the primer pair specific for *S. epidermidis* was used, an LDR product was found only from *S. epidermidis* (see Figure S4(D), Supporting Information). This indicated that *S. aureus* and *S. epidermidis* could be differentiated using LDR and strain-specific primers.

Fluorescence Resonance Energy Transfer (FRET)

To determine the optimal configuration of the rMB to maximize the FRET efficiency, LDR products were evaluated using bulk fluorescence measurements. In one LDR cocktail, 10 nM of the Cy5-labeled common primer and 10 nM of the Cy5.5-labeled discriminating primer were mixed with 100 nM of DNA target and subjected to 20 LDR thermal cycles. The high concentration of the target as well as the utilization of 20 thermal cycles made the rMB the dominant component in the reaction with most of the primers consumed following thermal cycling. In another LDR cocktail, the PCR template was not introduced so that only the primers were present following thermal cycling.

Figure 2A shows the emission spectra of the primer mixture without target. These spectra consisted of two features, one with an emission maximum around 664 nm corresponding to the Cy5-labeled primer and another feature with an emission maximum at ~700 nm associated with the Cy5.5-labeled primer, which appears as a weak shoulder on the major band seen at 664 nm. The fluorescence in this case originates primarily from direct excitation of the dye-labeled primers with the emission of Cy5 much higher than that of Cy5.5 because the excitation was set at Cy5's absorption maximum. When the temperature

was increased, the fluorescence of both dyes was found to decrease due to the temperature dependent fluorescence quantum yields associated with many carbocyanine dyes.³⁶

Figure 2B shows the emission spectra of the LDR cocktail containing the PCR template, which possessed a sequence complementary to the two primers. Compared to Figure 2A, the donor fluorescence was significantly reduced while the acceptor fluorescence increased. This indicated energy transfer between the donor and acceptor due to formation of the rMB structure. The efficiency of energy transfer was determined to be 42% at 70 °C according to the equation: $E_{\text{FRET}} = 1 - I_{\text{da}}/I_{\text{d}}$,³⁷ where I_{da} is the fluorescence of donor in the presence of acceptor, and I_{d} is the fluorescence of donor when acceptor was absent. When the temperature was increased from 50 to 70 °C, the fluorescence from both dyes decreased, similar to what was seen in Figure 2A. However, at a temperature of 90 °C, the acceptor fluorescence was completely absent in the emission spectrum. This was due to the temperature being set above the T_{m} of the stem structure of the rMB (83.4 °C), melting the duplexed DNA and, thus, spatially separating the donor from the acceptor dye, significantly reducing the energy transfer efficiency.

Effect of Linker Structure on FRET

To evaluate the efficiency of energy transfer between the donor and acceptor as a function of linker structure, different linkers were used for attaching the dye molecule to either the 3'- or 5'-ends of the oligonucleotide primers used for the LDR. Table S1 provides details of the linkers used for these investigations (see Supporting Information).

Figure 2C shows a comparison of the FRET emission from LDR products formed using primers with different linker structures (carbon spacer was either 3, 6, or 9 units). The shaded area indicates the detection window for registering acceptor fluorescence that was defined by the bandpass filter used for the LIF detector. The results indicated that using more than three carbon spacers for the linkers for both the discriminating and common primers produced lower acceptor fluorescence, suggesting reduced energy transfer efficiency. In FRET, the energy transfer efficiency, E_{FRET} , depends on the time-averaged spatial separation (R) between the donor and acceptor according to the Förster theory, given by $E_{\text{FRET}} = (1)/(1 + (R/R_{\text{O}})^6)$, where R_{O} is the Förster distance. The additional carbons used in the linkers resulted in larger time-averaged distance between the donor/acceptor pair compared to shorter carbon linkers;³⁸ it has been reported that the projection fluctuation of a 5-carbon linker is 0.9 nm versus 0.25 nm for a 2-carbon linker.³⁹ However, when the donor and acceptor are brought extremely close, they may also undergo static quenching.⁴⁰ Therefore, we engineered the LDR primers used to form the rMBs to possess a 3-carbon spacer on both ends to mitigate any possible quenching. On the basis of the data shown in Figure 2C, the optimal linker structure of those evaluated (see Table S2 of Supporting Information) consisted of a 3-carbon spacer used for both the donor and acceptor attachment to the 5'- and 3'-ends of the stem structures.

Single-Molecule Measurements of LDR-Generated rMBs Directly from Genomic DNA

Figure 3 shows single-molecule photon bursts from rMBs generated from a 20-cycle LDR performed on a COC microfluidic chip (see Figure S2, Supporting Information). The

reaction cocktail consisted of 10 pM of the common and discriminating primers in the presence of 6 copies/ nL of genomic DNA from *S. aureus*, *S. epidermidis*, and *E. coli*. The reaction mixture was driven at a volume flow rate of 0.78 $\mu\text{L}/\text{min}$, which was experimentally optimized to provide high single molecule signal-to-noise ratio and efficient LDR yields.⁴¹ From Figure 3, *S. aureus* resulted in clear single molecule signatures in the data trace, but when *S. epidermidis* or *E. coli* were present, no photon bursts from single molecules were detected. Because the LDR cocktail included primers specific for *S. aureus*, these results are consistent with the primers used for the LDR. We note that although the LDR primers contain complementary sequences even in the absence of ligation, the thermodynamic nature of the T_m for interstrand duplexes (i.e., nonligated primers) at pM concentrations are well below the detection temperature and, thus, no spFRET signal would be expected for unligated primers.³⁰ However, in the case of the ligated primers, which form intrastrand duplexes, the T_m is not concentration dependent.

To perform the thermally cycled LDR on a thermoplastic chip and detect single molecule events on the same chip, the substrate must have several important characteristics, including: (1) being chemically and thermally stable during the thermal cycling conditions required for the reaction; and (2) having low autofluorescence levels. In single-molecule measurements, COC is very attractive because it has excellent optical properties and extremely low fluorescence background in the near-IR region.⁴² Table S2 (Supporting Information) provides a comparison of autofluorescence levels for several commonly used thermoplastic materials. COC was used for all of the reported on-chip single-molecule measurements.

Single-molecule intensity histograms were analyzed for both background and samples containing the target bacterial species to set a threshold level to minimize errors due to false positive signals. Lower threshold levels reduce false negative errors but typically at the expense of increasing false positive errors. For the single-molecule histograms (data not shown), the average background fluorescence was determined to be ~ 1000 counts/s. When a threshold level was set at 3 times this average background level, there were no photon bursts detected from the blank, producing a false positive rate of 0 per data stream. At this threshold level, a total of 83 photon burst events were found for the positive control (see Figure 3).

For the bacterial genomes interrogated, the 16S rRNA gene appears in five locations. Considering the linear amplification associated with LDR and an average LDR efficiency of 40% per cycle, a 20-cycle LDR would generate 40 rMBs for each copy of genomic DNA. By driving the reaction mixture at 0.78 $\mu\text{L}/\text{min}$ and collecting data for 1 min, we would expect 187 200 rMBs flowing through the fluidic chip over this 1 min processing time. In the data trace of Figure 3A, 83 photon burst events were observed, which means that 0.04% of the rMBs were analyzed. For the LIF setup used herein, the probe volume can be approximated by a cylinder with a $1/e$ beam waist of the elliptical laser measured to be $2 \times 4 \mu\text{m}$. The height of the cylinder was determined by the size of the pinhole and estimated to be $\sim 2 \mu\text{m}$. Thus, the probe volume was estimated to be 12.6 fL, which yielded a single molecule sampling efficiency of 0.06%, which was obtained by dividing the probe volume ($\pi \times 1 \mu\text{m} \times 2 \mu\text{m} \times 2 \mu\text{m}$) by the cross sectional volume of the fluidic channel ($100 \mu\text{m} \times 100 \mu\text{m} \times 2 \mu\text{m}$). The experimentally observed sampling efficiency (0.04%) agreed

favorably with the percent of single rMBs calculated to travel through the probe volume with respect to the fluidic channel dimensions (0.06%).

Figure 4 shows a calibration plot of the number of detected photon burst events as a function of the input genomic DNA copy number. As can be seen, the calibration plot was linear ($r = 0.95$ for the 20-cycle LDR) over the copy numbers investigated. To examine if we could produce a shorter assay turnaround time, a 2-cycle LDR was also performed in the same COC chip with downstream single-molecule interrogation. The number of photon burst events was again linear with genomic DNA copy number with the slope of the calibration plot equal to 0.0032 photon bursts/ genomic DNA copy, compared to 0.015 photon bursts/ genomic DNA copy for the 20-cycle LDR. The slope describes the analytical sensitivity of the assay and the 20-cycle LDR was roughly 5 times more sensitive than the 2-cycle LDR. Clearly, the improved analytical sensitivity arose from increases in the number of cycles imposed on the LDR phase of the assay, which provides linear amplification of the number of rMB generated. However, the 20-cycle LDR reported results in 19.2 min, while the 2-cycle LDR produced results in 2.6 min.

In our case, the readout phases of the assay are instantaneous as the output from the continuous flow thermal reactor is sent directly into the fluorescence detector. As can be seen from the results depicted in Figure 4, the 20-cycle LDR can provide better analytical sensitivity in terms of discerning differences in copy numbers compared to the 2-cycle LDR. However, the photon bursts detected do originate from a single genomic DNA molecule but not as the input because the sampling efficiency is well below 100% and, thus, many DNA molecules are not detected due to the fact that they do not travel through the probe volume. To realize single copy detection as the input, the sampling efficiency must be increased to near 100%, which can be generated by reducing the geometrical dimensions of the fluidic channel where the laser-induced fluorescence detection occurs and/or by increasing the probe volume.

CONCLUSIONS

Results have been obtained demonstrating the capability of LDR/spFRET to provide a low limit-of-detection and rapid reporting of bacterial pathogens with strain specificity as well as the ability to distinguish Gram(+) from Gram(-) species. These measurements were performed directly within a COC microchip and demonstrated the ability to process the input DNA sample using LDR without a PCR amplification step and detect the products online in an automated fashion. With the measurements presented herein, the process time was found to be 2.6 min for a 2-cycle LDR and 19.2 min for a 20-cycle LDR. However, the larger number of cycles did improve the analytical sensitivity of the measurement. Significant improvements in assay sensitivity, even for the 2-cycle LDR, could be realized by simply increasing the sampling efficiency by reducing the channel size at the single-molecule detection zone of the chip and/or increasing the probe volume. For example, reducing the channel size to 1 μm (width) and 1 μm (depth) would provide a sampling efficiency of 100% for the laser beam size adopted herein.

The sampling rate, which is determined by the processing volume flow rate, must be balanced by optimizing the performance of the LDR³⁴ and the single-molecule detection efficiency.⁴¹ It was determined to be 0.078 $\mu\text{L}/\text{min}$ in the present case. This relatively low volumetric flow rate will make it difficult to process samples in which the bacterial copy number per unit volume is low, which would then require some type of bacterial target preconcentration prior to the LDR/spFRET measurement. This can be envisioned using an affinity preconcentrator that can process large input volumes and select targets with high recovery. We have recently demonstrated the ability to use polyclonal antibodies to select certain pathogenic bacteria that are of low abundance from water samples.⁴³ Future work in our laboratory will integrate this rare cell selection device to LDR/spFRET to provide the ability to identify rare bacterial species from environmental samples in near real-time.

Supplementary Material

Refer to Web version on PubMed Central for supplementary material.

Acknowledgments

We would like to thank the National Science Foundation (EPS-0346411) for financial support of this work as well as partial financial support through the World Class University (WCU) program of South Korea. The authors would also like to thank Mr. Jason Guy for his technical assistance in the microfabrication of the fluidic devices.

References

1. Chuang H, Macuch P, Tabacco MB. *Anal Chem.* 2001; 73:462–466. [PubMed: 11217747]
2. McDowell A, Mahenthalingam E, Moore JE, Dunbar KEA, Webb AK, Dodd ME, Martin SL, Millar BC, Scott CJ, Crowe M, Elborn JS. *J Clin Microbiol.* 2001; 39:4247–4255. [PubMed: 11724828]
3. Parkhurst DF, Stern DA. *Environ Sci Technol.* 1998; 32:3424–3429.
4. Alarcon B, Garcia-Canas V, Cifuentes A, Gonzalez R, Aznar R. *J Agric Food Chem.* 2004; 52:7180–7186. [PubMed: 15537335]
5. Belgrader P, Elkin CJ, Brown SB, Nasarabadi SN, Langlois RG, Milanovich FP, Colston BW, Marshall GD. *Anal Chem.* 2003; 75:3446–3450. [PubMed: 14570196]
6. Tang YW, Ellis NM, Hopkins MK, Smith DH, Dodge DE, Persing DH. *J Clin Microbiol.* 1998; 36:3674–3679. [PubMed: 9817894]
7. Rowe CA, Scruggs SB, Feldstein MJ, Golden JP, Ligler FS. *Anal Chem.* 1999; 71:433–439. [PubMed: 9949731]
8. Rowe CA, Tender LM, Feldstein MJ, Golden JP, Scruggs SB, MacCraith BD, Cras JJ, Ligler FS. *Anal Chem.* 1999; 71:3846–3852. [PubMed: 10489530]
9. Duburcq X, Olivier C, Malingue F, Desmet R, Bouzidi A, Zhou FL, Auriault C, Gras-Masse H, Melnyk O. *Bioconjugate Chem.* 2004; 15:307–316.
10. Delehanty JB, Ligler FS. *Anal Chem.* 2002; 74:5681–5687. [PubMed: 12433105]
11. Kim BC, Park JH, Gu MB. *Anal Chem.* 2005; 77:2311–2317. [PubMed: 15828762]
12. Lagally ET, Scherer JR, Blazej RG, Toriello NM, Diep BA, Ramchandani M, Sensabaugh GF, Riley LW, Mathies RA. *Anal Chem.* 2004; 76:3162–3170. [PubMed: 15167797]
13. Mayr BM, Kobold U, Moczko M, Nyeki A, Koch T, Huber CG. *Anal Chem.* 2005; 77:4563–4570. [PubMed: 16013874]
14. Loge FN, Thompson DE, Call DR. *Environ Sci Technol.* 2002; 36:2754–2759. [PubMed: 12099475]
15. Brasher CW, DePaola A, Jones DD, Bej AK. *Curr Microbiol.* 1998; 37:101–107. [PubMed: 9662609]

16. Kong RYC, Lee SKY, Law TWF, Law SHW, Wu RSS. *Water Res.* 2002; 36:2802–2812. [PubMed: 12146868]
17. Beyor N, Yi LN, Seo TS, Mathies RA. *Anal Chem.* 2009; 81:3523–3528. [PubMed: 19341275]
18. Zourob M, Mohr S, Brown BJT, Fielden PR, McDonnell MB, Goddard NJ. *Anal Chem.* 2005; 77:232–242. [PubMed: 15623301]
19. Zourob M, Hawkes JJ, Coakley WT, Brown BJT, Fielden PR, McDonnell MB, Goddard NJ. *Anal Chem.* 2005; 77:6163–6168. [PubMed: 16194074]
20. Premasiri WR, Moir DT, Klempner MS, Krieger N, Jones G, Ziegler LD. *J Phys Chem B.* 2005; 109:312–320. [PubMed: 16851017]
21. Jarvis RM, Goodacre R. *Anal Chem.* 2004; 76:40–47. [PubMed: 14697030]
22. Tok JBH, Chuang FYS, Kao MC, Rose KA, Pannu SS, Sha MY, Chakarova G, Penn SG, Dougherty GM. *Angew Chem, Int Ed.* 2006; 45:6900–6904.
23. Weeks BL, Camarero J, Noy A, Miller AE, Stanker L, De Yoreo JJ. *Scanning.* 2003; 25:297–299. [PubMed: 14696978]
24. Campbell GA, Mutharasan R. *Biosens Bioelectron.* 2005; 21:462–473. [PubMed: 16076436]
25. Gupta AK, Nair PR, Akin D, Ladisch MR, Broyles S, Alam MA, Bashir R. *Proc Natl Acad Sci USA.* 2006; 103:13362–13367. [PubMed: 16938886]
26. Rider TH, Petrovick MS, Nargi FE, Harper JD, Schwoebel ED, Mathews RH, Blanchard DJ, Bortolin LT, Young AM, Chen JZ, Hollis MA. *Science.* 2003; 301:213–215. [PubMed: 12855808]
27. Van Ert MN, Easterday WR, Simonson TS, U'Ren JM, Pearson T, Kenefic LJ, Busch JD, Huynh LY, Dukerich M, Trim CB, Beaudry J, Welty-Bernard A, Read T, Fraser CM, Ravel J, Keim P. *J Clin Microbiol.* 2007; 45:47–53. [PubMed: 17093023]
28. Pingle MR, Granger K, Feinberg P, Shatsky R, Sterling B, Rundell M, Spitzer E, Larone D, Golightly L, Barany F. *J Clin Microbiol.* 2007; 45:1927–1935. [PubMed: 17428930]
29. Barany F. *Proc Natl Acad Sci USA.* 1991; 88:189–193. [PubMed: 1986365]
30. Wabuyele MB, Farquar H, Stryjewski W, Hammer RP, Soper SA, Cheng YW, Barany F. *J Am Chem Soc.* 2003; 125:6937–6945. [PubMed: 12783546]
31. Gill SR, Fouts DE, Archer GL, Mongodin EF, DeBoy RT, Ravel J, Paulsen IT, Kolonay JF, Brinkac L, Beanan M, Dodson RJ, Daugherty SC, Madupu R, Angiuoli SV, Durkin AS, Haft DH, Vamathevan J, Khouri H, Utterback T, Lee C, Dimitrov G, Jiang LX, Qin HY, Weidman J, Tran K, Kang K, Hance IR, Nelson KE, Fraser CM. *J Bacteriol.* 2005; 187:2426–2438. [PubMed: 15774886]
32. Krimmer V, Merkert H, von Eiff C, Frosch M, Eulert J, Lohr JF, Hacker J, Ziebuhr W. *J Clin Microbiol.* 1999; 37:2667–2673. [PubMed: 10405419]
33. Chen JF, Wabuyele M, Chen HW, Patterson D, Hupert M, Shadpour H, Nikitopoulos D, Soper SA. *Anal Chem.* 2005; 77:658–666. [PubMed: 15649068]
34. Hashimoto M, Hupert ML, Murphy MC, Soper SA, Cheng YW, Barany F. *Anal Chem.* 2005; 77:3243–3255. [PubMed: 15889915]
35. Clarridge JE. *Clin Microbiol Rev.* 2004; 17:840–862. [PubMed: 15489351]
36. Mali KS, Dutt GB, Mukherjee T. *J Chem Phys.* 2008; 128:1–9.
37. Chen Y, Mauldin JP, Day RN, Periasamy A. *J Microsc (Oxford).* 2007; 228:139–152. [PubMed: 17970914]
38. Ha T, Enderle T, Ogletree DF, Chemla DS, Selvin PR, Weiss S. *Proc Natl Acad Sci USA.* 1996; 93:6264–6268. [PubMed: 8692803]
39. Best RB, Merchant KA, Gopich IV, Schuler B, Bax A, Eaton WA. *Proc Natl Acad Sci USA.* 2007; 104:18964–18969. [PubMed: 18029448]
40. Marras SAE, Kramer FR, Tyagi S. *Nucleic Acids Res.* 2002; 30:e122. [PubMed: 12409481]
41. Mathies RA, Peck K, Stryer L. *Anal Chem.* 1990; 62:1786–1791. [PubMed: 2240569]
42. Okagbare PI, Emory JM, Datta P, Goettert J, Soper SA. *Lab Chip.* 2010; 10:66–73. [PubMed: 20024052]
43. Dharmasiri U, Witek MA, Adams AA, Osiri JK, Hupert ML, Bianchi TS, Roelke DL, Soper SA. *Anal Chem.* 2010; 82:2844–2849. [PubMed: 20218574]

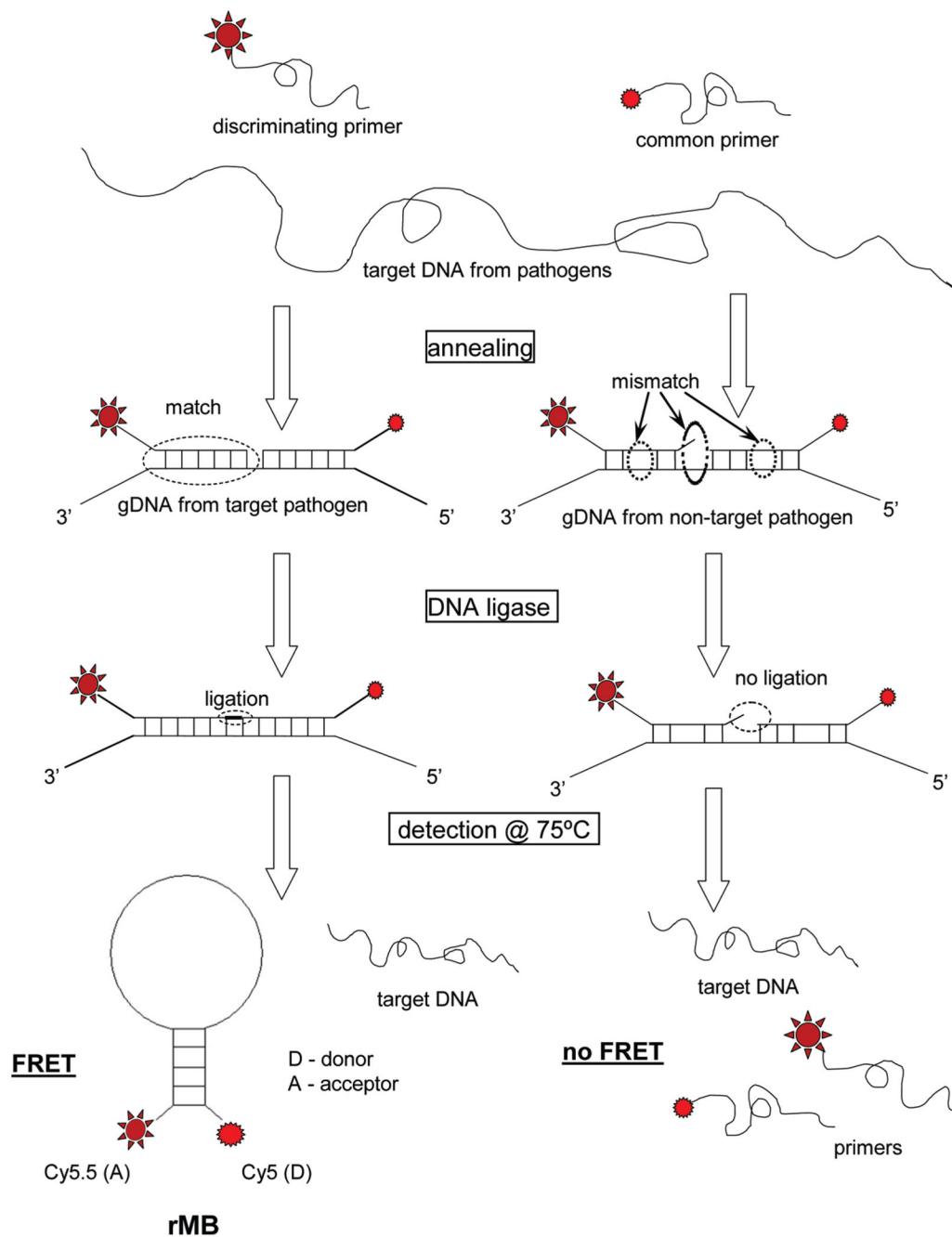


Figure 1. Illustration of the LDR-spFRET assay. A discriminating primer and a common primer were designed based on the sequence of a reporter region within the genome of a target pathogen. The discriminating and common primers each contained a 10-base arm with complementary sequences that were end labeled with a donor or an acceptor fluorophore, respectively, to report spFRET when a reverse molecular beacon (rMB) was formed. In the presence of a target DNA, the two primers hybridized to the target and were covalently joined by a ligase enzyme to form a longer oligonucleotide strand only if the primers were completely

complementary to the target. The arm sequences of the rMB were designed to be thermodynamically more stable than the DNA target-oligonucleotide duplex. Thus, the rMB reorganized itself into a stable stem-loop conformation. In this stem-loop structure, energy from the donor was transferred to the acceptor due to FRET, indicating a successful LDR event.

Author Manuscript

Author Manuscript

Author Manuscript

Author Manuscript

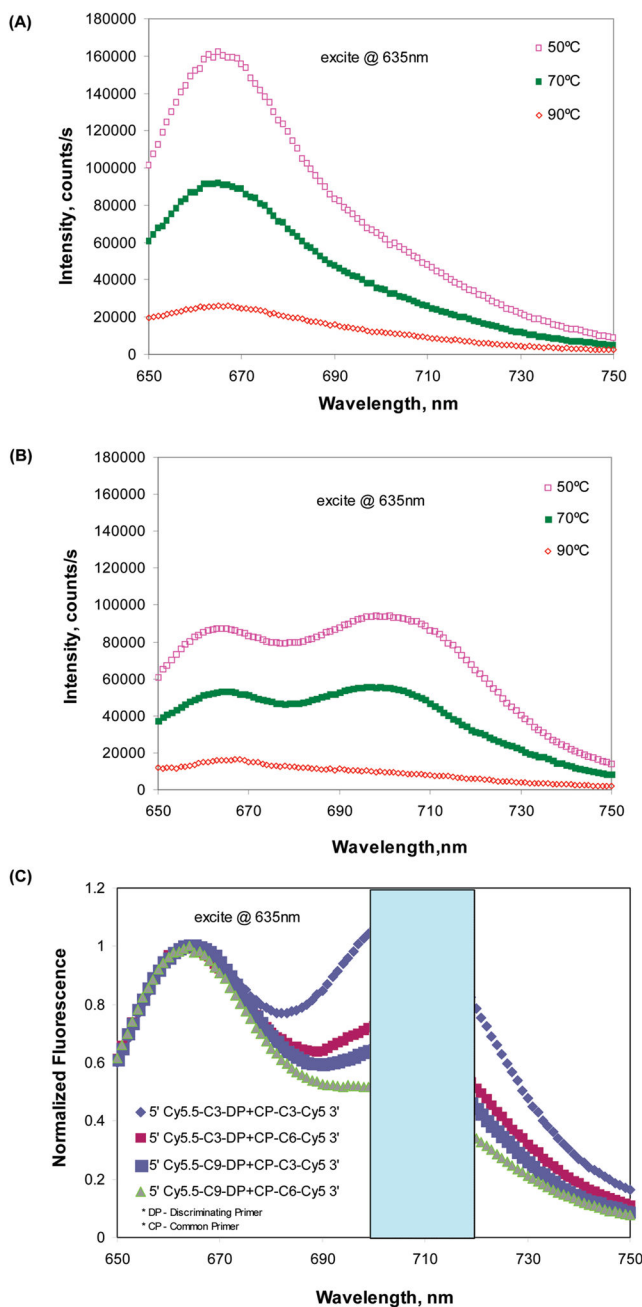


Figure 2. Measurements showing the emission spectra of the donor/acceptor dye pair of the rMB for FRET verification. (A) Emission spectra of a mixture of dye-labeled primers (10 nM each) after 20 LDR thermal cycles in the absence of the DNA target. (B) Emission spectra of LDR dye-labeled primers (10 nM of each primer) and 1 nM of the target DNA following 20-LDR thermal cycles. (C) Emission spectra of LDR products after 20-LDR thermal cycles using primers with different linkers used to attach the donor/acceptor dyes to the primer. The shaded area in (C) indicates the detection window used in the LIF detector for monitoring

acceptor fluorescence. See Table S1 in the Supporting Information for the structure of the chemical linkers.

Author Manuscript

Author Manuscript

Author Manuscript

Author Manuscript

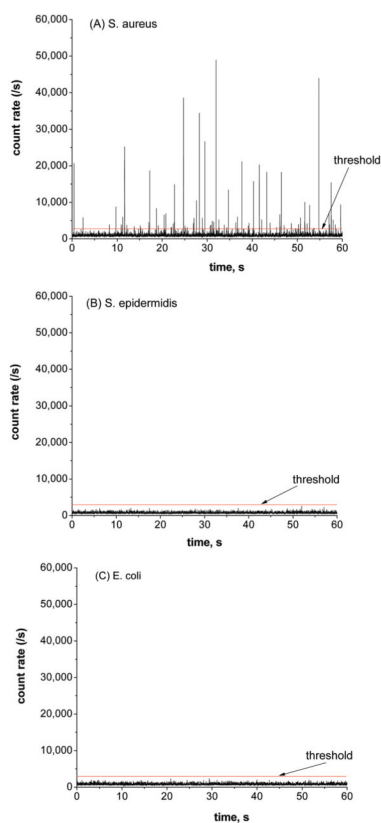


Figure 3.

Single-molecule photon bursts of LDR-generated rMBs. LDR was performed on the COC microfluidic chip using a continuous flow process. (A) Photon bursts generated from *S. aureus* genomic DNA; (B) photon bursts from *S. epidermidis* genomic DNA; and (C) photon bursts from *E. coli* targets. The reaction cocktail consisted of 10 pM of the common and discriminating primers as well as 6 copies/ nL of genomic DNA from *S. aureus*, *S. epidermidis*, and *E. coli*. A 20-cycle LDR was run for all three bacteria on the COC microchip. When analyzing the data, a threshold of 3000 counts/s was used to discriminate the single-molecule events from background fluorescence.

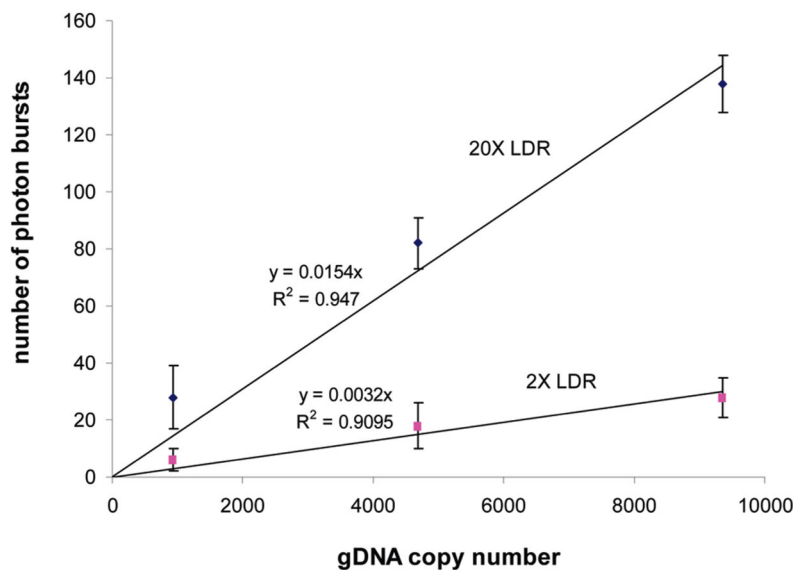


Figure 4.

Plot of the number of detected photon burst events versus the input genomic DNA copy number. The upper curve shows the linear fit to a 20-cycle LDR with a correlation coefficient of 0.95, and the lower curve shows the fit to a 2-cycle LDR with a correlation coefficient of 0.91. The slope of the linear fitting function for the 2-cycle LDR was 0.0032, compared to 0.015 for the 20-cycle LDR. The slope of the fitting line described the sensitivity of the assay; the 20-cycle LDR was ~5 times more sensitive than the 2-cycle LDR.

Table 1

Oligonucleotide Sequences Used as the PCR and LDR Primers for the Strain-Specific Identification of Bacterial Species

	primers	sequence (5'-3')^a
PCR primers	AMP1 forward	ACTGAGACACGGTCCAGACTCCTAC
	AMP1 reverse	GTAGCGGTGAAATGCGCAGAGATA
	AMP2 forward	CAAACAGGATTAGATACCCTGGTAGTC
	AMP2 reverse	GAAGGTGGGGATGACGTCAAAT
	Gram(+) disc	Cy5.5-C3- <u>AGGCGGCGCG</u> AGCGAAAGCCTGACGGAGCA
Gram(+) com	p ^b ACGCCGCGTGAGTGATGAAGGT <u>ACGCGCCGCCT</u> -C3-Cy5	
LDR primers	<i>S. aureus</i> disc	Cy5.5-C3- <u>AGGCGGCGCG</u> TTACCAAATCTTGACATCCTTTGACA
	<i>S. aureus</i> com	pACTCTAGAGATAGAGCCTTCCCCTTCGG <u>CGCGCCGCCT</u> -C3-Cy5
	<i>S. epid</i> disc	Cy5.5-C3- <u>AGGCGGCGCG</u> CGTAAAACCTCTGTTATTAGGGAAGAACAA
	<i>S. epid</i> com	pATGTGTAAGTAACTATGCACGTCTTGAC <u>GC</u> CGCCGCCT-C3-Cy5

^aThe underlined sequence consists of the stem of the rMB, which is formed following ligation. In all cases, a 3-carbon linker was used to attach the donor or acceptor to the oligonucleotides to maximize energy transfer efficiencies (see Table S1, Supporting Information, and Figure 2C).

^bp, phosphorylation.